



Gas Sensing Properties of Nanosized $\text{Mg}_{0.2}\text{Cd}_{0.8}\text{Al}_2\text{O}_4$ based Thick Film Sensor

S.V. Agnihotri^{1*} and V.D. Kapse²

¹Department of Physics, Arts, Commerce and Science College, Kiran Nagar, Amravati 444606, Maharashtra State, India

²Department of Physics, Arts, Science and Commerce College, Chikhaldara 444807, Maharashtra State, India
srta.ashish@rediffmail.com

Available online at: www.isca.in, www.isca.me

Received 2nd October 2016, revised 14th November 2016, accepted 17th November 2016

Abstract

Nanocrystalline $\text{Mg}_{0.2}\text{Cd}_{0.8}\text{Al}_2\text{O}_4$ has been successfully synthesized by co precipitation method. The materials were investigated for structural properties by X-ray diffraction (XRD), Fourier transforms infrared spectroscopy (FT-IR) and Scanning electron microscopy with dispersive analysis (SEM-EDAX). LPG sensing properties of $\text{Mg}_{0.2}\text{Cd}_{0.8}\text{Al}_2\text{O}_4$ were investigated at room temperature. Further the sensor was observed selective at an optimal operating temperature (338 K). The sensor was found to be stable and repeatable with good response and recovery time. The gas sensing mechanism of $\text{Mg}_{0.2}\text{Cd}_{0.8}\text{Al}_2\text{O}_4$ has been discussed elaborately.

Keywords: Magnesium aluminate, Gas sensor, Screen printing, X-ray diffraction Nanoparticles.

Introduction

Semiconductor metal oxides (SMO) have received increasing attention due to their unique physical properties. Metal oxide materials have an excellent surface property so they are used for the detection of inflammable gases and for hydrocarbons. The SMO based gas sensors have numerous advantages, such as small sizes, high sensitivities in detecting very low concentrations of a wide range of gaseous chemical compounds, possibility of on-line operation and, due to possible bench production, low cost. These advantages attracted great interest of industrial and scientific world. In SMO sensor, gas is sense due to chemical interaction between the gas molecules and surface film. Thick film of number of material including single- (ZnO , SnO_2 , In_2O_3 , WO_3 , TiO_2 , Fe_2O_3) and multi component oxides- (BiFe_2O_3 , MgAl_2O_4 , CoAl_2O_4 , SrTiO_3 , ZnAl_2O_4) have shown significant results as regards to gas sensing properties. A spinel is a ternary oxide. It has a chemical formula AB_2O_4 in which 'A' stands for a divalent metallic cation at a tetrahedral site and 'B' for trivalent metallic cation at an octahedral site of the cubic structure. High resistance to chemical attack, good mechanical strength from room temperature to high temperatures, low dielectric constant, excellent optical properties, low thermal expansion and good catalytic properties are seen in magnesium aluminate spinel¹⁻⁵. Thick films are fabricated by screen printing, tape casting, dip coating process. Thick film gas sensors fabricated by using screen-printing technique have numerous advantages over other types of gas sensors. They are low cost, small size, simple construction, and have good sensing properties and robust chemical sensor with good reproducibility⁶⁻⁸. The present study deals with the gas sensing properties of $\text{Mg}_{0.2}\text{Cd}_{0.8}\text{Al}_2\text{O}_4$.

Materials and Methods

Preparation of nanocrystalline $\text{Mg}_{0.2}\text{Cd}_{0.8}\text{Al}_2\text{O}_4$: In today's world, demands for detection and controlling production of hazardous and noxious gases have become the issue of great concern for the mankind due to growing concern about environment protection and security.

Nanocrystalline $\text{Mg}_{0.2}\text{Cd}_{0.8}\text{Al}_2\text{O}_4$ was prepared by dissolving appropriate amounts of magnesium nitrate [$\text{Mg}(\text{NO}_3)_2$], aluminium nitrate [$\text{Al}(\text{NO}_3)_3$] and cadmium nitrate [$\text{Cd}(\text{NO}_3)_2$] in distilled water. The mixture was kept under continuous stirring at 353 K for 1 h. The proper amount of aqueous ammonia solution (25 wt. %) was poured drop wise in the above mixture, and then the solution was stirred until complete precipitation occurred. The obtained precipitate was filtered, washed with distilled water and ethanol for several times. The precipitate was dried out for 24 h at 383 K. The dry precipitate was calcinated at 1073 K for 4 h to obtain $\text{Mg}_{0.2}\text{Cd}_{0.8}\text{Al}_2\text{O}_4$ nanoparticles.

Material characterizations: The characterization of the powder was carried out by X-ray diffraction (XRD) and Fourier transforms infrared spectroscopy (FTIR). Infrared spectra were recorded (3000 Hyperion microscope) 1 wt.% weight sample in KBr. The morphology of the film was characterized by scanning electron microscopy (JEOL JSM 7600F) with dispersive analysis (SEM-EDAX). The structural characterization of the powders was made by X-ray diffraction (XRD) at room temperature, The XRD patterns were recorded on X-ray diffractometer (PANalytical X'Pert-Pro) using a Cu-K_α mono chromatized radiation source and a filtered in the range $2\theta = 10-$

90°. The crystallite sizes of the spinel powder were calculated from line-broadening, using Scherer's equation⁹

$$D = 0.9\lambda / \beta \cos\theta$$

Where, D stands for crystallite size, λ for the wavelength of incident X-rays (0.15405 nm), β for the peak width at half height and θ corresponds to the peak position.

Thick film sensor fabrication and measurement of gas-sensing properties: As prepared powders were grounded with α terpineol, ethyl-cellulose and 2(2-butoxyethoxy) ethyl acetate in order to get the paste. Pastes incorporating mass percentage ratio of 70:30, with $Mg_{0.2}Cd_{0.8}Al_2O_4$ and the binder respectively were ground in an agate pestle and mortar with for 1 h. This paste was screen printed onto glass substrate surface of size 25 mm x 25 mm. This film was allowed to dry for 24 h at room temperature and heat treatment was given to the film at 626 K for 2 h. For surface resistance measurement, the electrodes of silver were deposited on adjacent sides of the film and then it was kept to heating at 353 K for 15 min for drying the silver paint. The sensing response was determined from resistance change of thick film sensor.

The films thickness was obtained in the range 25 to 30 mm The thickness of the film was maintained by proper rheology and thixotropy of the paste, The 'static gas-sensing system' was used to obtain the gas sensing performance. There were electrical feeds through the base plate. The heater was placed on the base plate. This arrangement heat up the sample to check require operating temperatures. By using adjustable ON and OFF time intervals relay, the current passing through the heating element was measured. With Cr-Al thermocouple the operating temperature of the sensor was sensed. The output of the thermocouple was coupled with digital temperature indicator. At one of the ports of the base plate gas inlet valve was fixed. The required amount of gas concentration was achieved by injecting

a sufficient volume of test gas using a gas-injecting syringe inside the static system. The sensor response is defined as¹⁰,

$$S = \frac{\Delta R}{R_a} = \frac{|R_g - R_a|}{R_a} \times 100\%$$

Where: R_a is the resistance of the sensor measured in the air and R_g is the resistance in the presence of the target gas.

Selectivity is defined as, 'the ability of a sensor element to respond to specific target gas in the presence of other gases'. Also response time is defined as, 'the time taken for the sensor to attain the maximum (90%) change in conductance on exposure to the target gas is measured'. The time taken by the sensor to regain 90% of the original value is the recovery time. The sensor selectivity has been determined by placing different contaminants in the test chamber with high accuracy chromatographic syringes. The selectivity of the sensors to that LPG, CH_4 and CO_2 can be calculated.

Results and Discussion

X-Ray diffraction (XRD): The X-ray diffraction pattern of $Mg_{0.2}Cd_{0.8}Al_2O_4$ powder calcinated at 1073 K for 4 h is shown in Figure-1. It was found that the structure of the material is spinel phase. Each one of the diffraction peaks can be absolutely indexed to cubic spinel-structured. The appearance of very sharp and narrow peaks also signifies the presence of very small crystallite size in the calcined powder. With the help of peak broadening relation, the crystallite size and diffraction angle can be calculated. The average crystallite size of $Mg_{0.2}Cd_{0.8}Al_2O_4$ powder is about 9.1 nm.

Fourier transforms infrared resonance spectroscopy (FTIR): FTIR spectrum is calculated in the regions 400–4000 cm^{-1} of wide and spiky bands in diverse frequency range with the units of reciprocal centimetres (cm^{-1}).

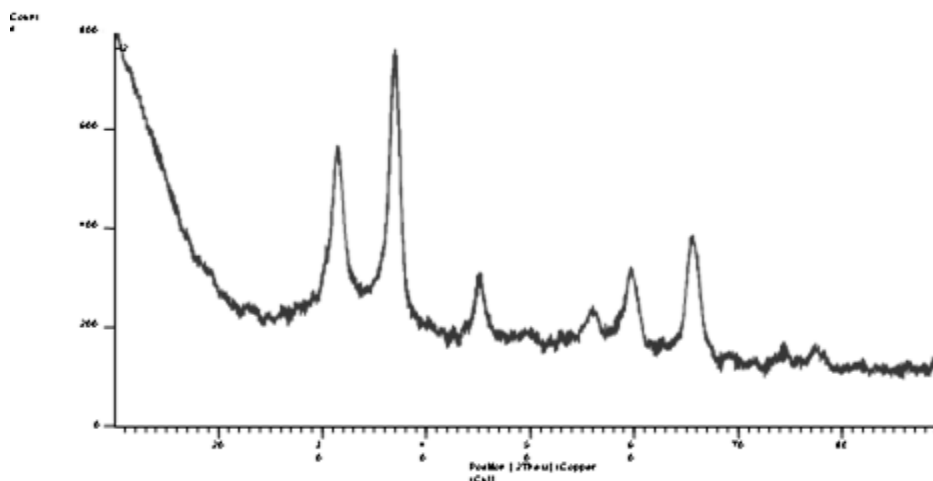


Figure-1
XRD patterns of sample after calcinations process

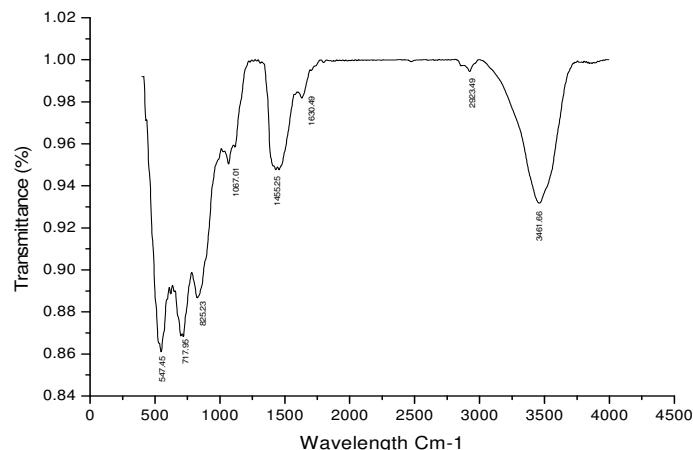


Figure-2

FTIR Spectra of $\text{Mg}_{0.2}\text{Cd}_{0.8}\text{Al}_2\text{O}_4$ after calcinations process

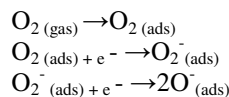
The FT-IR spectrum of the sample shows the rapid adsorption of H_2O and CO_2 molecules from the atmosphere which possesses the large specific surface area. The peaks at 3461.66 cm^{-1} may be observed due to the stretching vibration of H_2O molecules, whereas the H_2O bending occurs at 1630.49 cm^{-1} band. The stretching vibration of CO_2 because of the absorption band at 2923.51 cm^{-1} . The peaks obtained at 717.95 , 621.40 and 547.45 cm^{-1} confirm the formation of normal spinel structure¹¹⁻¹².

Scanning Electron Microscopy with electron dispersive analysis (SEM-EDAX): The surface morphology of magnesium doped with cadmium aluminate thick film, visualized by means of Scanning Electron Micrographs (SEM), is shown in Figure-3. The surface morphology of the film can be clear from the scanning electron micrographs (SEM). The SEM images of the film propose moderately fine particle size distributions. The SEM shows some particles are in the 25-29 nm range and few agglomerates are produced. Particular elements and their relative proportions can be identified with the Energy Dispersive X-ray analysis. The wt% of MgK (1.83), AlK (29.72), CdK (19.33) presents in the EDAX image, shown in Figure-4.

The Gas sensing properties: The response of $\text{Mg}_{0.2}\text{Cd}_{0.8}\text{Al}_2\text{O}_4$ thick film sensors to various concentrations of LPG, CO_2 and CH_4 are measured. The operating temperature affects the sensor response to LPG gas. As shown in Figure-5, the sensor starts sensing LPG at about 300 K and reaches a maximum of 11.03 at about 338 K. Sensitivity is steeply reduced with the increasing operating temperature in the range of 348 to 398 K.

Response of the $\text{Mg}_{0.2}\text{Cd}_{0.8}\text{Al}_2\text{O}_4$ thick film sensor fabricated in this work was found to enhance with rising temperature. At a particular temperature the sensor response is maximum. Gas sensing phenomenon depends on electron transfer reaction. When the reducing gas molecules interact with the adsorbed oxygen existing on $\text{Mg}_{0.2}\text{Cd}_{0.8}\text{Al}_2\text{O}_4$ thick film sensor surface which leads to the remarkable fall in the value of R_g , giving

maximum sensing response. When the reducing gas species and chemisorbed oxygen are interact with each other the electron carrier concentration of sensing $\text{Mg}_{0.2}\text{Cd}_{0.8}\text{Al}_2\text{O}_4$ layer increase followed by releasing the trapped electrons. The increase in the concentration of electron in the conduction band of $\text{Mg}_{0.2}\text{Cd}_{0.8}\text{Al}_2\text{O}_4$ layer occurs because of the fall in sensor resistance (R_g) in the presence of reducing gas. Above mechanism for adsorbed oxygen species occurs as follows,



The interactions between LPG and adsorbed oxygen ions are,

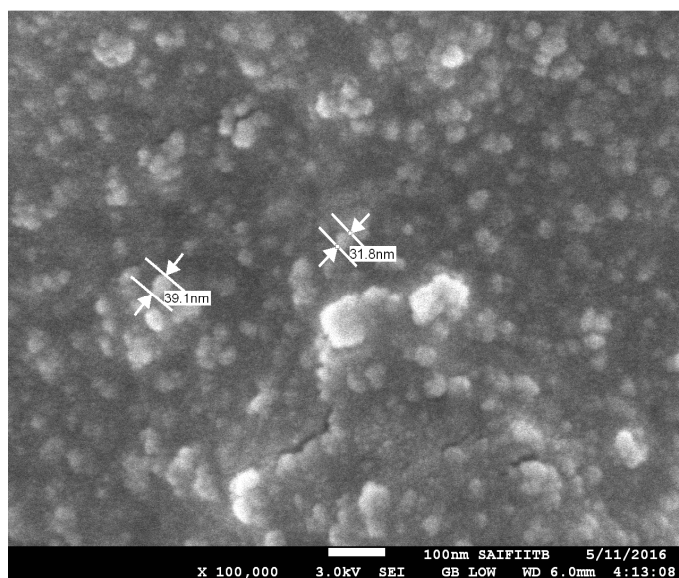
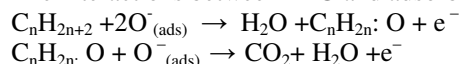


Figure-3

Scanning electron micrograph of $\text{Mg}_{0.2}\text{Cd}_{0.8}\text{Al}_2\text{O}_4$ thick film

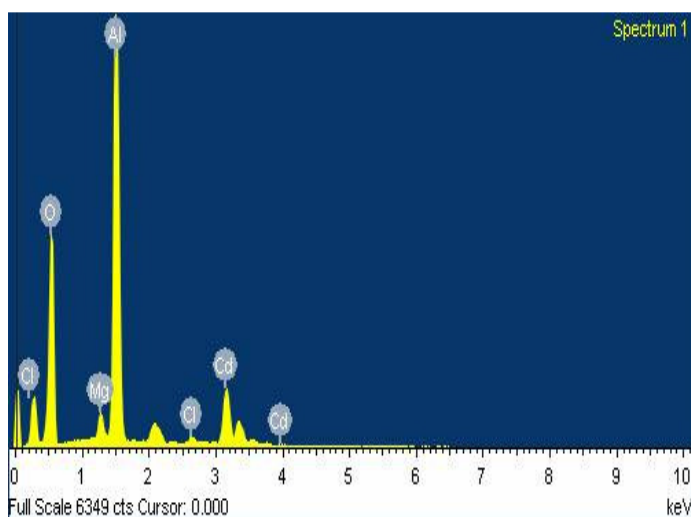


Figure-4

EDAX of $\text{Mg}_{0.2}\text{Cd}_{0.8}\text{Al}_2\text{O}_4$ thick film

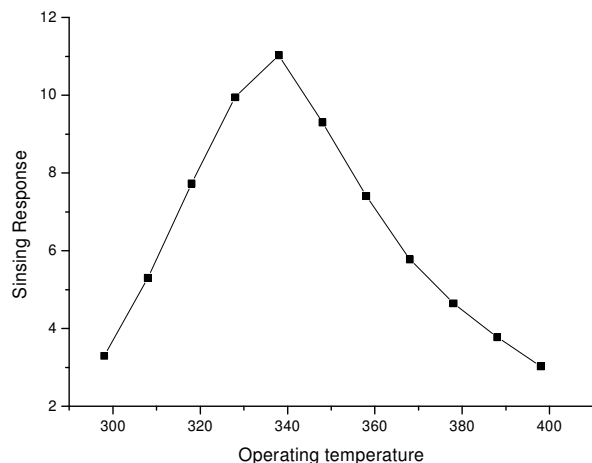


Figure-5

Curve between operating temperature and sensor response

Moreover, the sensitivity of $\text{Mg}_{0.2}\text{Cd}_{0.8}\text{Al}_2\text{O}_4$ based sensor was measured for 500 ppm of liquefied petroleum gas at room temperature for 30 days. The result was illustrated in Figure-6. It was found that the sensor response almost constant for 30 days, indicating good stability. The results showed that the sensor based on nanocrystalline $\text{Mg}_{0.2}\text{Cd}_{0.8}\text{Al}_2\text{O}_4$ was stable for LPG sensing.

The response time and recovery time are the two main sensing parameters of gas sensor. Figure-7 depicts the graph of response and recovery time of the gas sensor when it was exposed to 500 ppm LPG at 303 K. When the LPG gas was passed through the chamber, the resistance of the sensor enhanced, the sensor response time was 60 s. As soon as the LPG gas was taken out, the resistance improved quickly and the recovery time found to be 30 s. As a result of this the sensor shows the better response and recovery characteristics.

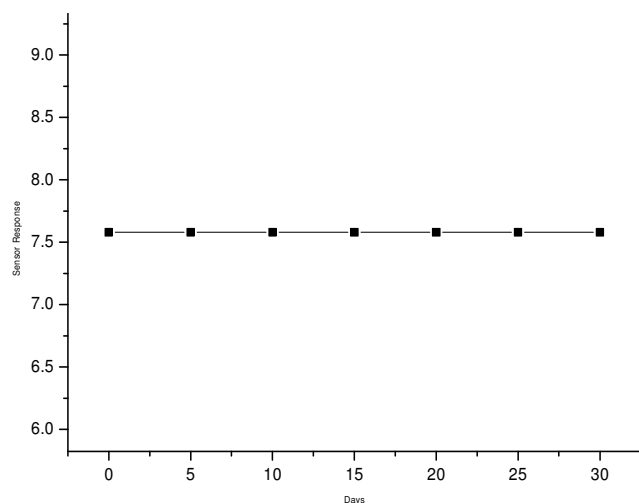


Figure-6

Long term stability curve of $\text{Mg}_{0.2}\text{Cd}_{0.8}\text{Al}_2\text{O}_4$ thick film sensor

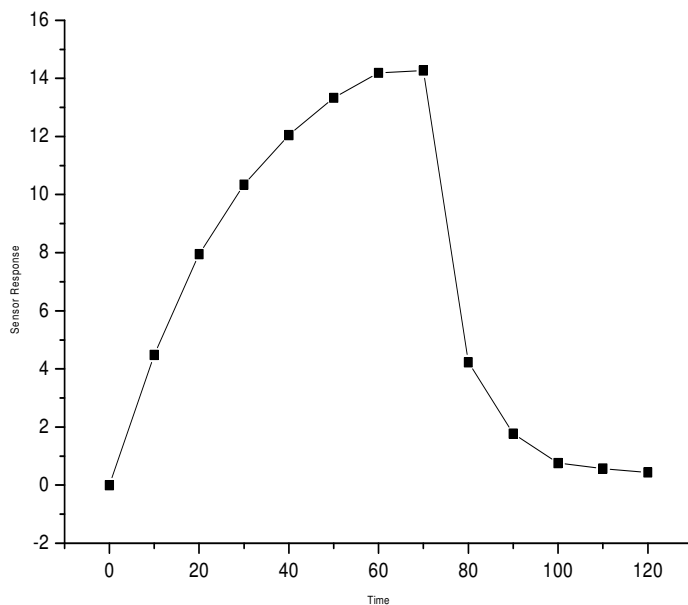


Figure-7

Response and recovery characteristics of $\text{Mg}_{0.2}\text{Cd}_{0.8}\text{Al}_2\text{O}_4$ thick film sensor at 500 ppm LPG

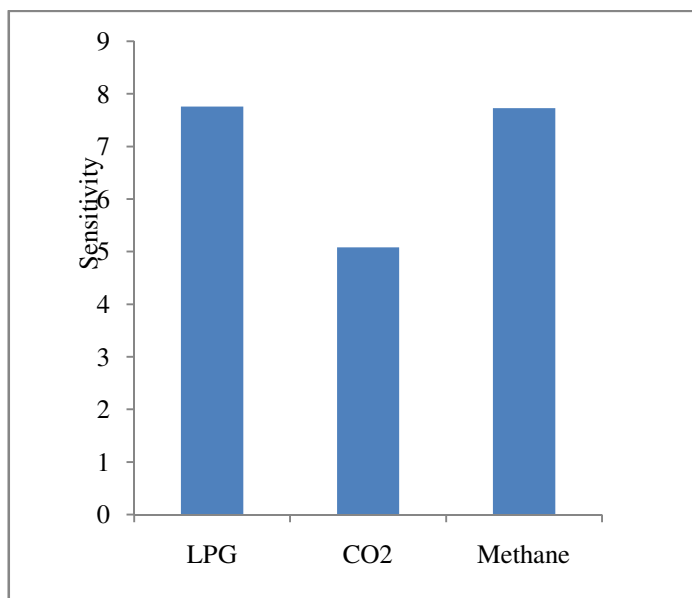


Figure-8

Response of $\text{Mg}_{0.2}\text{Cd}_{0.8}\text{Al}_2\text{O}_4$ sensor to different gases

Selectivity is one of the significant characteristics of gas sensors. The $\text{Mg}_{0.2}\text{Cd}_{0.8}\text{Al}_2\text{O}_4$ thick film sensor was exposed to several gases at the concentration of 500 ppm with the optimum operating temperatures. Figure-8 shows $\text{Mg}_{0.2}\text{Cd}_{0.8}\text{Al}_2\text{O}_4$ sensor response towards LPG, CO_2 and CH_4 . LPG is a composition of CH_4 , C_3H_8 and C_4H_{10} . So $\text{Mg}_{0.2}\text{Cd}_{0.8}\text{Al}_2\text{O}_4$ sensor had high response towards LPG and CH_4 as compared to CO_2 . Investigations are necessary to enhance selectivity of $\text{Mg}_{0.2}\text{Cd}_{0.8}\text{Al}_2\text{O}_4$ towards LPG.

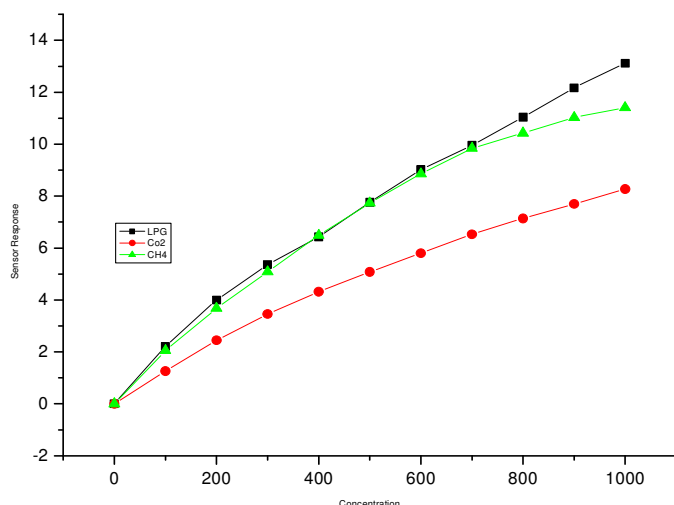


Figure-9

Concentration Vs response of $\text{Mg}_{0.2}\text{Cd}_{0.8}\text{Al}_2\text{O}_4$ sensor at 296

Figure-9 depicts the sensor response of the $\text{Mg}_{0.2}\text{Cd}_{0.8}\text{Al}_2\text{O}_4$ thick film sensor versus the concentration of LPG, CO_2 and CH_4 . From the figure it can be clear that the curve is linear. The sensor response of 1000 ppm LPG is maximum at 13.12, which is greater than the sensor response of 1000 ppm CO_2 , and CH_4 . Selectivity of $\text{Mg}_{0.2}\text{Cd}_{0.8}\text{Al}_2\text{O}_4$ thick film sensor towards LPG is greater than CO_2 and CH_4 gases.

Conclusion

Semi conductive $\text{Mg}_{0.2}\text{Cd}_{0.8}\text{Al}_2\text{O}_4$ was synthesized by co precipitation method. After that calcinations done at 1073 K for 4 h. The XRD analysis confirms the spinel phase formation of $\text{Mg}_{0.2}\text{Cd}_{0.8}\text{Al}_2\text{O}_4$ composite. FT-IR spectra ensured the vibrational stretching frequencies analogous to the composites. $\text{Mg}_{0.2}\text{Cd}_{0.8}\text{Al}_2\text{O}_4$ has good response and recovery characteristics hence it can also be used as a LPG sensor. The image of SEM showed that the $\text{Mg}_{0.2}\text{Cd}_{0.8}\text{Al}_2\text{O}_4$ as synthesized using high amounts of cadmium has a significant porosity. The $\text{Mg}_{0.2}\text{Cd}_{0.8}\text{Al}_2\text{O}_4$ thick film sensor showed considerable response and selectivity towards LPG working at 303 K. The selectivity coefficient to LPG of sensor was measured at the optimum working temperature. This new approach enriches the preparation method of $\text{Mg}_{0.2}\text{Cd}_{0.8}\text{Al}_2\text{O}_4$ and brings new opportunity for the application of $\text{Mg}_{0.2}\text{Cd}_{0.8}\text{Al}_2\text{O}_4$ nanostructure as gas sensors. It can be considered for using as selective gas-sensing material to LPG.

Acknowledgements

The authors thank to Sophisticated Analytical Instrument Facility, Chandigarh, for providing XRD facility. A special thanks to S.A.I.F., Indian Institute of Technology, Bombay for carrying out FT-IR and SEM-EDAX.

References

1. Nuernberg G.B., Foletto E.L., Campos C., Fajardob H., Carreno N. and Probst L. (2012). Direct decomposition of methane over Ni catalyst supported in magnesium aluminate. *J. Power Sour*, 208, 409–414.
2. Saito F. and Kim W. (1999). A review on magnesium aluminate (MgAl_2O_4) spinel synthesis. *Powder Technol*, 113, 109–113.
3. Dung T.W., Ping L.R. and Azad A.M. (2001). Magnesium aluminate (MgAl_2O_4) via self-heat-sustained (SHS) technique. *Mater. Res. Bull*, 36, 1417–1430.
4. Mazzoni A.D., Sainz M.A., Caballero A. and Aglietti E.F. (2002). Formation and sintering of spinels (MgAl_2O_4) in reducing atmosphere. *Mater Chem Phys*, 78, 30–37.
5. Bocanegra S.A., Ballarini A.D., Scelza O.A. and Miguel S.R. (2008). The influence of the synthesis routes of as support of dehydrogenation catalyst. *Mater. Chem Phys*, 111, 534–541.
6. Noh W., Shin Y., Kim J., Lee W., Hong K., Akbar S.A. and Park J. (2002). Surface morphology and sensing property of NiO-WO_3 Thin film. *Solid State Ionics*, 152-153, 827–832.
7. Carotta M.C., Martinelli G., Sadaoka Y., Nunziante P. and Traversa E. (1998). Environmental monitoring field tests using screen-printed thick-film. *Sens. Actuators B Chem.*, 48, 270–276.
8. Guidi V., Butturi M.A., Carotta M.C., Cavicchi B., Ferroni M., Malagu C., Martinelli G., Vincenzi D., Sacerdoti M. and Zen M. (2002). Solide state gas sensor. *Sens. Actuat. B Chem.* 84, 72-77.
9. Kong L. and Shen Y. (1996). Gas sensing property and mechanism of $\text{Ca}_x\text{La}_{1-x}\text{FeO}_3$ ceramic. *Sens. and Actuat. B* 30, 217–221.
10. Llobet E., Ivanov P., Vilanova X., Brezmes J., Hubalek J., Malysz K.I., Gràcia I., Cané C. and Correig X. (2003). Screen-printed nanoparticle tin oxide films for high-yield sensor microsystems. *Sens. and Actuat. B Chem*, 96, 1- 2, 94-104.
11. Olhero S.M., Ganesh I., Torres P.M.C. and Ferreira J.M.F. (2008). Surface passivation of MgAl_2O_4 spinel powder by chemisorbing H_3PO_4 for easy aqueous processing. *Langmuir*, 24, 9525–9530.
12. Puriwat J., Chaitree W., Suriye K., Dokjampa S., Praserttham P. and Panpranot J. (2010). Elucidation of the basicity dependence of 1-butene isomerization on MgO/Mg(OH)_2 catalysts. *Catal. Commun.*, 12, 80–85.